# **Characterization of Staggered Twin Formation in HCP Magnesium**

M. Arul Kumar, B. Leu, P. Rottmann, and I. J. Beyerlein

#### Abstract

Twins in hexagonal close-packed polycrystals, most often nucleate at grain-boundaries (GBs), propagate into the grain and terminate at opposing GBs. Regularly, multiple parallel twins of the same variant form inside the same grain. When twins terminate inside the grains, rather than the grain boundary, they tend to form a staggered structure. Whether a staggered twin structure or the more common grain spanning twin structure forms can greatly affect mechanical behavior. In this work, the underlying mechanism for the formation of staggered twins is studied using an elasto-visco-plastic fast Fourier transform model, which quantifies the local stresses associated with  $\{10\overline{1}2\}$ -type staggered twins in magnesium for different configurations. The model results suggest that when a twin tip is close to the lateral side of another twin, the driving force for twin propagation is significantly reduced. As a result, the staggered twin structure forms.

### **Keywords**

Deformation twins • Staggered structure • Local stresses • Crystal plasticity • Magnesium

M. Arul Kumar (⊠)

Los Alamos National Laboratory, Materials Science and Technology Division, Los Alamos, NM 8745, USA e-mail: marulkr@lanl.gov

B. Leu · P. Rottmann · I. J. Beyerlein Materials Department, University of California at Santa Barbara, Santa Barbara, CA 93106, USA

#### L. J. Beverlein

Mechanical Engineering Department, University of California at Santa Barbara, Santa Barbara, CA 93106, USA

## Introduction

Deformation twinning in hexagonal close-packed (HCP) metals, particularly in magnesium and its alloys, is a prevalent deformation mechanism due to the scarcity of relatively easy dislocation slip modes [1-3]. Unlike slip, a deformation twin forms as a lamellar domain with significant lattice reorientation relative to the parent crystal and local shear [4–6]. For instance,  $\{10\overline{1}2\}$  tensile twin in HCP Mg reorients the crystal by 86.3° with 12.6% local shear [2]. The crystallography and morphology of deformation twin can therefore be easily seen in microscopy techniques like electron backscatter diffraction (EBSD) and transmission electron microscopy (TEM) [4, 5, 7, 8]. Based on the loading condition with respect to c-axis of the crystal, different twinning modes can be formed. For example, tensile twins  $\{10\overline{1}2\}$  and  $\{11\overline{2}1\}$  form when the loading condition extends the crystal along the c-axis, and compression twins  $\{11\overline{2}2\}$  and  $\{10\overline{1}1\}$ form when the loading condition results in contraction of the c-axis [1–3]. Among all possible twinning modes, the  $\{10\overline{1}2\}$ tensile twin type is the most frequent one in HCP Mg and it is considered in this article [4].

Most deformation twins in polycrystals nucleate at grain boundaries, where stress concentrations and a high density of defects are both located [4, 6, 9, 10]. Successfully formed twin embryos propagate into the grain and terminate at the opposing grain boundaries. Under further straining, twins can continue to propagate across the grain boundaries and develop twin chains [4, 11] or they can expand in size by thickening. Often, multiple twins form inside a grain, which leads to either parallel twins or twin–twin junction microstructure [4, 12]. Every twinning microstructure affects the material behavior differently. For example, parallel twins increase the density of barriers for dislocation motion [13, 14]. Twin–twin junctions can increase the local strain hardening rate as well as act as preferential sites for damage nucleation [15, 16].

Recently, we have observed a staggered twin microstructure in HCP magnesium. This type of structure is frequently seen but has not received much attention to date. The EBSD and scanning TEM images of a particular Mg grain that shows the staggered twin structure is shown in Fig. 1a and b, respectively. Similar to parallel twin configuration, staggered twin structure also increases the density of barriers for dislocation motion and so increases the grain size induced strain hardening behavior. In this case, AZ31 Mg polycrystal with an initial basal texture compressed along the rolling direction to 2% engineering strain. It imposes tension along the c-axis for most of the grains and thus leads to the activation of tensile twin. Here, the twin tips of staggered twins have terminated inside the grain and not at the grain boundary. This situation differs from the typical one in which twins would very easily and relatively rapidly propagate in the crystal compared to the time scales of slip [17, 18]. As a result, twins frequently terminate at the opposing grain boundaries and hence fully span the grain [4, 6]. Thus, by comparison, the formation of staggered twin structures, wherein the twin tips terminate in the crystal, implies a significant departure in the usual twinning dynamics. Currently, is it not clear how a staggered twin configuration would develop.

In this work, we employ a crystal plasticity-based micromechanical model to study how stable staggered twinning microstructure could be formed. Using a full-field elasto-visco-plastic Fast Fourier Transform model, we calculate the local stresses at the tips of an isolated and staggered set of twins. The stress calculations show that the presence of an adjacent staggered twin decreases the driving stress for twin tip propagation. Thus, for similar defect configuration, the twin propagation rate will be lower for staggered twins compared to isolated twins. This may be the reason for the stable staggered twin structure observed in an HCP Mg crystal. The understanding of underlying physical

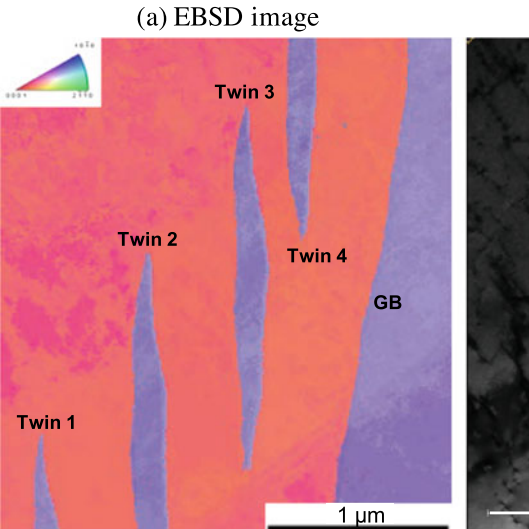
mechanisms for staggered twin formation could pave a platform for designing controlled in situ experiments to characterize the local stresses at the twin tips. Twins that terminate at grain boundaries restrict the characterization of local stresses at the twin tips and twin propagation process.

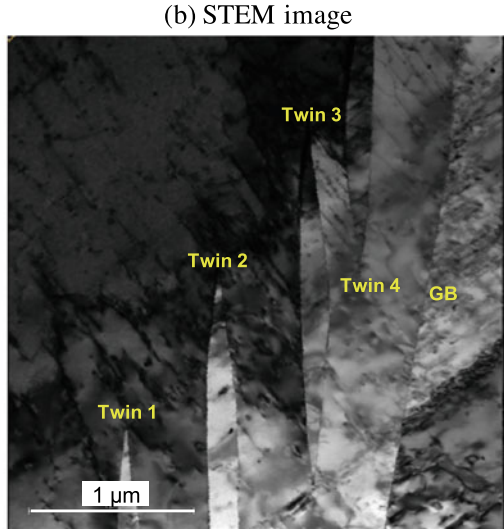
### **Numerical Method: FFT Model**

To calculate the local stresses around twin tips, we employ a version of a full-field, elasto-visco-plastic Fast Fourier Transform (EVP-FFT) model that has been advanced to treat discrete twin lamella [12, 19]. The original FFT formulation was developed to study the local and effective mechanical response of composite materials [20, 21]. Later, Lebensohn [22] adapted it for polycrystalline materials to study the effective and local responses associated with the heterogeneity in the spatial distribution of crystallography and directional dependence of mechanical properties. This basic FFT formulation has been extended to different deformation regimes like elasticity [23], incompressible visco-plasticity [22, 24], dilatational visco-plasticity [25], infinitesimal elasto-visco-plasticity [26, 27] and finite elasto-viscoplasticity [28]. The current EVP-FFT version used here incorporates the twin transformation strain in regions predefined with a twin orientation. It has been successfully applied to study neighboring grain and grain size effect on twin growth, parallel twin formation and twin transmission across grain boundaries [11, 12, 29–31].

The twin FFT model builds upon an infinitesimal elasto-visco-plasticity formulation. Within this framework, the deformation twin is a domain that undergoes a shear transformation. Taken together, the constitutive behavior for an elasto-visco-plastic material under an infinitesimal strain approximation including the shear transformation is given by

Fig. 1 Experimentally observed staggered {1012} tensile twin microstructure in HCP magnesium. a, b EBSD and STEM image of part of the twinned grain that shows staggered twins





$$\sigma(x) = \mathbf{C}(x) : \boldsymbol{\varepsilon}^{e}(x) = \mathbf{C}(x) : (\boldsymbol{\varepsilon}(x) - \boldsymbol{\varepsilon}^{p}(x) - \boldsymbol{\varepsilon}^{tr}(x))$$
 (1)

In the above expression,  $\sigma(x)$  is the Cauchy stress tensor, C(x) is the elastic stiffness tensor,  $\epsilon(x)$ ,  $\epsilon^e(x)$ , and  $\epsilon^p(x)$  are the total, elastic and plastic strain tensors, and  $\epsilon^{tr}$  is the transformation strain. The local stress field at a material point x is solved using an implicit time discretization of the form:

$$\begin{split} \boldsymbol{\sigma}^{t+\Delta t}(\boldsymbol{x}) &= \boldsymbol{C}(\boldsymbol{x}) : \left( \boldsymbol{\epsilon}^{t+\Delta t}(\boldsymbol{x}) - \boldsymbol{\epsilon}^{p,t}(\boldsymbol{x}) - \dot{\boldsymbol{\epsilon}}^{p,t+\Delta t}(\boldsymbol{x}) \Delta t - \boldsymbol{\epsilon}^{tr,t}(\boldsymbol{x}) - \Delta \boldsymbol{\epsilon}^{tr,t+\Delta t}(\boldsymbol{x}) \right) \end{split} \tag{2}$$

Within the twin domain, twin transformation strain is imposed. To build up the twinning transformation, successive shear increments are imposed within the twin domain using the following strain increments:

$$\Delta \boldsymbol{\epsilon}^{tr}(\mathbf{x}) = \mathbf{m}^{tw}(\mathbf{x}) \Delta \boldsymbol{\gamma}^{tw}(\mathbf{x}) \tag{3}$$

For material points outside the twin domains,  $\Delta \epsilon^{tr}(x)$  is zero. The tensor  $\mathbf{m}^{tw} = \frac{1}{2}(\mathbf{b}^{tw} \otimes \mathbf{n}^{tw} + \mathbf{n}^{tw} \otimes \mathbf{b}^{tw})$  is the Schmid tensor associated with the twin system, where  $\mathbf{b}^{tw}$  and  $\mathbf{n}^{tw}$  are unit vectors along the twinning direction and the twin plane normal, respectively. The number of increments  $N^{twincr}$  needed to reach the characteristic twinning shear,  $s^{tw}$  is simply:

$$\Delta \gamma^{\text{tw}}(\mathbf{x}) = \frac{\mathbf{s}^{\text{tw}}}{\mathbf{N}^{\text{twiner}}} \tag{4}$$

In the following calculations, we set the time increment  $\Delta t$  and  $N^{twincr}$  sufficiently low and high, respectively, to ensure convergence.

## **FFT Simulation Details**

In this work, we study the role of local stresses on stable staggered twin formation. To clearly understand the effect of twins' interaction on local stresses and then on its propagation, we simulate different staggered twin configurations. We also consider the stress field around an isolated twin as a reference. To simplify the analysis, the calculations are performed within a single grain and any effects from neighboring grains are neglected. Figure 2 shows a schematic representation of the simulation setup for (a) an isolated twin and (b) staggered twin structure. This setup consists of one orientation (grain) finely discretized, surrounded by a buffer layer consisting of 20,000 voxels, with each voxel being assigned a randomly generated orientation. While one may regard this layer as an effective surrounding medium, the simulations that we present here treat the central part as the representative volume and are not affected by the details of the buffer construction. The unit cell is

discretized into  $510 \times 510$  voxels and has three voxels in the X-direction. This thickness is determined to be sufficient for capturing the spatially resolved stress distribution and is unaffected by this boundary cell size.

For the calculations, we select the crystallographic orientation of the grain to be  $(0^{\circ}, 0^{\circ}, 0^{\circ})$ , in the Bunge convention, which corresponds to alignment of the  $\begin{bmatrix} 10\overline{1}0 \end{bmatrix}$  and  $\begin{bmatrix} 0001 \end{bmatrix}$  axes parallel to the Y- and Z-directions, respectively. The unit cell is subjected to compression along the Y-direction, and thus gives a high Schmid factor ( $\sim 0.5$ ) for the  $(10\overline{1}2)[\overline{1}011]$  twin variant, lying in the Y-Z plane. Due to this geometry, there is no out-of-plane twin shear in the X-Y and X-Z planes. The twin domain in the simulation is assumed to have elliptical shape with an aspect ratio of 25. The minor axis is spanned by eight voxels for both the isolated and staggered twin pairs. The inclination of the twinning plane with respect to the compression axis is  $\pm 43.1^{\circ}$ .

Figure 2 shows the model staggered twin pair. These two twins are positioned with a spacing s and relative inclination  $\theta$ . To study the effect of the relative arrangement of twins on their local stresses, we systematically vary the spacing s and relative inclination  $\theta$  and in each case calculate the resolved shear stresses along the twin boundary.

The stress state corresponds to the equilibrium state. For a given configuration of twins, we perform the following sequence of steps to achieve equilibrium. First, the entire unit cell is compressed along the Y-direction under a constant applied strain rate to 0.001 strain (compressive stress in Y-direction is  $\sim 40$  MPa). This imposes compression normal to the c-axis (or tension along the c-axis), which replicates the experimental condition. This imposed strain induces a positive resolved shear stress (RSS) of  $\sim 20$  MPa. This value is of the order of a critical threshold of the twin resolved shear stress for  $\{10\overline{1}2\}$  twining in Mg [32]. Second, the discrete twin(s) is/are introduced, by reorienting the crystal on those voxels pre-selected for the twin domain and enforcing twinning transformation shear in several increments. During these steps, the externally imposed strain is fixed.

At all stages in the simulation, the deformation is accommodated by elastic and plastic deformation. The constitutive law material parameters used in simulations are the elastic moduli tensor, the plastic slip modes, and the CRSS values for activating them. For pure Mg, the elastic constants at room temperature used are:  $C_{11} = 58.58$ ,  $C_{12} = 25.02$ ,  $C_{13} = 20.79$ ,  $C_{33} = 61.11$  and  $C_{44} = 16.58$  GPa [33, 34]. Plasticity is accommodated by three slip modes: basal <a>, prismatic <a>, and pyramidal <c + a> II slip and the corresponding CRSS values are: 3.3, 35.7 and 86.2 MPa, respectively [32]. In these calculations, we expect that work hardening and lattice rotations will be negligible since the calculations involve only a few percent

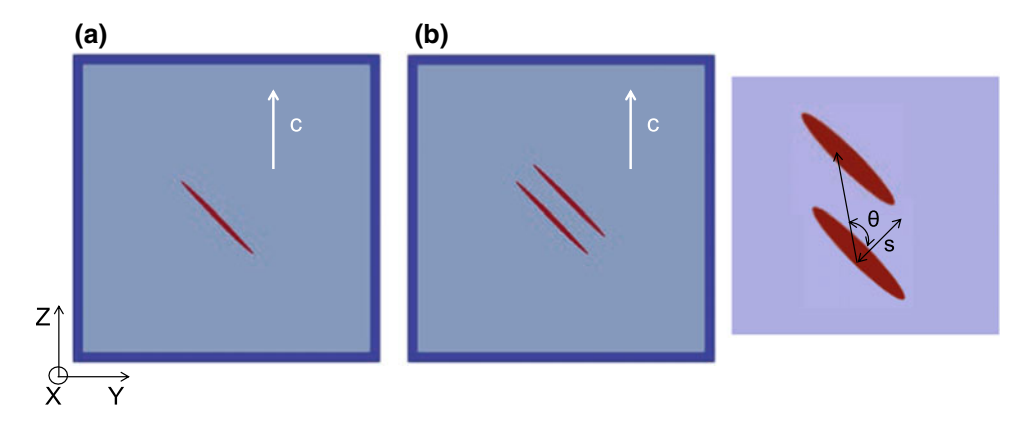


**Fig. 2** EVP-FFT model setup for isolated and staggered twins simulations. **a**  $\{10\overline{1}2\}$  tensile twin inside a grain, which is surrounded by a buffer that represents the polycrystal with uniform crystal

orientation distribution. The grain orientation is  $((0^o,0^o,0^o))$  in Bunge convection, which aligns the grain c-axis with Z-direction. **b** Staggered twins of same type and variant with spacing s and relative inclination  $\theta$ 

macroscopic strains. Therefore, a constant, non-evolving CRSS value for slip on each slip system will be employed in the calculations here. However, should larger macroscopic strains be desired, hardening effects could easily be considered in this model framework.

## **Results and Discussion**

The EVP-FFT model calculations provide complete stress, elastic and plastic strain tensors and other micromechanical fields at every material point (i.e. voxel). Among all the stress components, the resolved shear stress on the twin plane along the twin direction (TRSS) is a key variable for twin propagation and thickening. For the analysis in this study, the TRSS fields are evaluated. As mentioned early, we first consider the stress fields around an isolated twin as a reference case. Figure 3a shows the TRSS fields around the isolated twin, and it is highly heterogenous. Note that the TRSS before twinning is positive and homogenous everywhere in the simulation cell. Twin formation results in significantly heterogeneous stress fields. Particularly, the constraint for twinning shear induces a TRSS reversal (i.e. blue, negative TRSS) within and in the vicinity of twin; see Fig. 3a. The amount of stress reversal could be viewed as a twin back stress, since it acts in the sense that opposes twinning and restricts further twin thickening process. Contrary to stress reversal in the twin domain, we observe a stress concentration at the twin tips and its sense favors further forward twin propagation. This high-stress concentration at twin tips, referred as a forward stress, supports the experimentally observed "self-catalytic" tendency of twin propagation in crystals; i.e., twin propagation unhindered across the crystal. Considering the twin in isolation does not explain how a staggered twin structure would be mechanically stable.

To understand the formation and stability of stagger twinning microstructure, we have performed similar local stress calculations for staggered twin configurations varying in s and  $\theta$  (see Fig. 2b). As we have seen in Fig. 3a, the stress field generated around a twin is highly heterogenous and the stress reversal region formed around the twin extends distances several times the twin thickness and decaying in magnitude with the distance from the twin. Another twin identical in crystallography and size would interact with this twin, particularly if it were located within this region. Next, we repeat the calculations for two staggered twins, in which their spacing s lay within this region. Figure 3b and c shows the calculated TRSS fields for the case of s = 4t,  $\theta = 0^{\circ}$  and s = 4t,  $\theta = 40^{\circ}$ , respectively, where t is the twin thickness. By comparing the TRSS fields of isolated and staggered twin cases, we can immediately confirm that their stress fields differ from that of the isolated twin, indicating that they have been altered by the twin-twin interaction. First, the resolved twin shear stress along their lateral twin boundaries is, like the isolated twin, directed in the anti-twinning sense but, compared to the isolated twin, even more intense. Hence, this staggered twin configuration would tend to stunt their thickening. For forward propagation (lengthening), the stress concentration at the twin tip is important. We find that the stress concentration at the staggered twin tips is significantly different from that of the isolated twin tips.

As a measure of twin tip stress concentration, we calculate the average TRSS in the stress concentrated volume  $\Omega$  ahead of the twin tip (see insert in Fig. 4). The average TRSS values at the two tips of the isolated twin are 41.18 and 41.17 MPa. Similarly, the average TRSS values at the tips of T1, T2, T3 and T4 belonging to the staggered twin pair with s = 4t,  $\theta = 0^{\circ}$  (see Fig. 4 insert) are 23.81, 21.25, 21.30 and 23.82 MPa, respectively. These values are

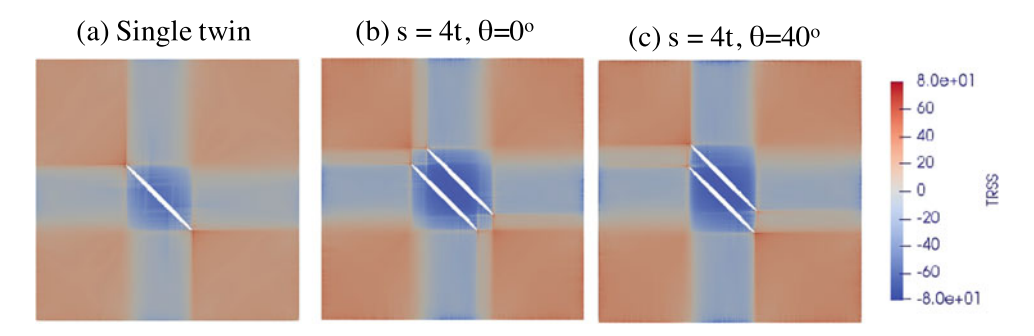


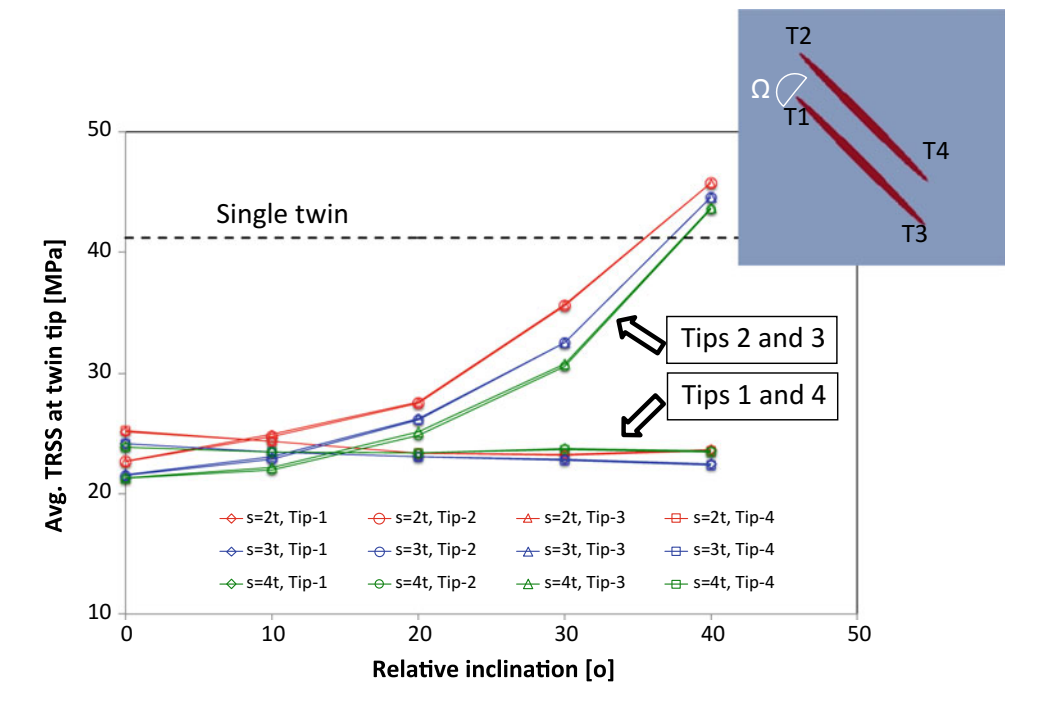
Fig. 3 TRSS distribution for a isolated twin and for closely spaced twins with  $\mathbf{b}$  s = 4t and  $\theta$  = 0° and  $\mathbf{c}$  s = 4t and  $\theta$  = 40°. The closely spaced twins interact and alter the TRSS fields in the vicinity of each twin, particularly at the twin tips

significantly lower than that of isolated twin case, which suggests that the driving force for further twin propagation is lower for all the tips of staggered twins compared to isolated twin. To study the effect of the staggered twin geometry, we calculate the average TRSS at the twin tips for different spacings (s = 2t, 3t and 4t) and relative inclinations ( $\theta = 0$ ,  $10^{\circ}$ ,  $20^{\circ}$ ,  $30^{\circ}$  and  $40^{\circ}$ ). The results are plotted in Fig. 4 along with isolated twin case for comparison. For all values of s, we observe a similar trend with respect to  $\theta$ . The effect of the twin interaction decreases with increasing relative inclination  $\theta$  for the tips that are "away" from the interaction region (T2 and T3), but not for the tips that are "inside" the interaction region (T1 and T4). For  $\theta > 30^{\circ}$ , the twin forward stress at tips T2 and T3 are comparable to those of the isolated twin case. Consequently, we can expect that the driving force for twin propagation will be lower for the twins that are sufficiently close, specifically lying within the twin

interaction region. Due to the staggered configuration, the staggered twin microstructure cannot undergo propagation at the same rate as that of the isolated twin.

Characterizing both the local microstructure and micromechanical fields at the twin tips and twin interfaces is essential for understanding the propagation and thickening processes of twins. Several experimental efforts using high-resolution microscopy and/or X-ray diffraction techniques have recently focused on twin interfaces and the effect of paired twin interactions on subsequent twin boundary migration [8, 35–40]. However, to date, similar in situ tests have not yet been performed for twin tips and their relation to twin propagation, likely because twin propagates rapidly due to the high driving force at the twin tips. Results of this work on stagger twin formation suggest that the twin tip propagation rate can be controlled by the nearby twinning microstructure. With this in mind, one

Fig. 4 Changes in the average TRSS at the twin tip as a function of twin spacing, s, and relative inclination,  $\theta$ . The interaction between closely placed twins lowers the TRSS at the twin tips, and so twin propagation may be delayed. Thus, it may lead to stable staggered twinning microstructure formation



could think on an interesting set of in situ experiments for characterizing the motion of twin tips. For instance, we propose the following possible design for controlled in situ experiments. (1) Prepare either micropillar samples or TEM thin foil samples from the bulk polycrystal such that they contain a pre-existing twin. If this sample is subjected to a loading that favors twinning, then pre-existing twins can thicken or a new twin can be formed if the appropriate stress and/or defect concentrations are present [41, 42]. It can, however, be difficult to anticipate the twin nucleation site for these samples. Introduction of a geometrical perturbation, like a notch, near the pre-existing twin before applying the load could help to nucleate a new twin preferably at this site. The local micromechanical fields associated with the pre-existing twin will control the propagation rate of the newly formed twin. This approach permits monitoring and characterizing the twin propagation process dynamically.

## Summary

In this work, for the first time, we have investigated the underlying mechanisms for staggered twin structure formation. The interaction of nearby twins affects the local stresses associated with individual twins. In particular, the driving force for twin propagation at the twin tips is substantially reduced due to the local twin–twin interaction compared to that for the tip of an isolated twin. Thus, the propagation rate of a pair of staggered parallel twins will be lowered, and the likelihood of stabilizing a staggered twin structure will be enhanced. Based on this finding, we have proposed a possible design for a controlled experiment that would enable characterization of twin propagation by closely monitoring the twin tips.

Acknowledgements This work is fully funded by the US Department of Energy, Office of Basic Energy Sciences Project FWP 06SCPE401. I.J.B. acknowledges financial support from the National Science Foundation (NSF CMMI-1729887). BL acknowledges financial support from the National Defense Science and Engineering Graduate (NDSEG) Fellowship. The authors thank Luoning Ma (Johns Hopkins University) for the preparation of TEM specimen.

## References

- P.G. Partridge (1967) The crystallography and deformation modes of hexagonal close-packed metals. Metallurgical Reviews 12: 169–194.
- M.H. Yoo (1981) Slip, Twinning, and Fracture in Hexagonal Close-Packed Metals. Metall Trans A 12(3): 409–418.
- M.H. Yoo, J.K. Lee (1991) Deformation Twinning in Hcp Metals and Alloys. Philos Mag A 63(5): 987–1000.
- I.J. Beyerlein, L. Capolungo, P.E. Marshall, R.J. McCabe, C.N. Tome (2010) Statistical analyses of deformation twinning in magnesium (vol 90, pg 2161, 2010). Philos Mag 90(30): 4073–4074.

- L. Capolungo, P.E. Marshall, R.J. McCabe, I.J. Beyerlein, C.N. Tome (2009) Nucleation and growth of twins in Zr: A statistical study. Acta Mater 57(20): 6047–6056.
- M.A. Kumar, M. Wroński, R.J. McCabe, L. Capolungo, K. Wierzbanowski, C.N. Tomé (2018) Role of microstructure on twin nucleation and growth in HCP titanium: A statistical study. Acta Mater 148: 123–132.
- R.J. McCabe, G. Proust, E.K. Cerreta, A. Misra (2009) Quantitative analysis of deformation twinning in zirconium. Int J Plasticity 25(3): 454–472.
- B.M. Morrow, R.J. Mccabe, E.K. Cerreta, C.N. Tome (2014) In-Situ TEM Observation of Twinning and Detwinning During Cyclic Loading in Mg. Metall Mater Trans A 45a(1): 36–40.
- J. Wang, I.J. Beyerlein, C.N. Tome (2010) An atomic and probabilistic perspective on twin nucleation in Mg. Scripta Mater 63(7): 741–746.
- J. Wang, J.P. Hirth, C.N. Tome (2009) ((1)over-bar0 1 2) Twinning nucleation mechanisms in hexagonal-close-packed crystals. Acta Mater 57(18): 5521–5530.
- M.A. Kumar, I.J. Beyerlein, R.J. McCabe, C.N. Tome (2016) Grain neighbour effects on twin transmission in hexagonal close-packed materials. Nat Commun 7.
- M.A. Kumar, I.J. Beyerlein, C.N. Tome (2016) Effect of local stress fields on twin characteristics in HCP metals. Acta Mater 116: 143–154.
- G.C. Kaschner, C.N. Tome, I.J. Beyerlein, S.C. Vogel, D.W. Brown, R.J. McCabe (2006) Role of twinning in the hardening response of zirconium during temperature reloads. Acta Mater 54 (11): 2887–2896.
- G. Proust, C.N. Tome, G.C. Kaschner (2007) Modeling texture, twinning and hardening evolution during deformation of hexagonal materials. Acta Mater 55(6): 2137–2148.
- Q. Yu, J. Wang, Y.Y. Jiang, R.J. McCabe, N. Li, C.N. Tome (2014) Twin-twin interactions in magnesium. Acta Mater 77: 28–42.
- Q. Yu, J. Zhang, Y. Jiang (2011) Fatigue damage development in pure polycrystalline magnesium under cyclic tension–compression loading. Materials Science and Engineering: A 528(25–26): 7816–7826.
- N.P. Daphalapurkar, J.W. Wilkerson, T.W. Wright, K.T. Ramesh (2014) Kinetics of a fast moving twin boundary in nickel. Acta Mater 68: 82–92.
- E. Faran, D. Shilo (2010) Twin Motion Faster Than the Speed of Sound. Phys Rev Lett 104(15).
- M.A. Kumar, A.K. Kanjarla, S.R. Niezgoda, R.A. Lebensohn, C. N. Tome (2015) Numerical study of the stress state of a deformation twin in magnesium. Acta Mater 84: 349–358.
- J. Michel, H. Moulinec, P. Suquet (2000) A computational method based on augmented Lagrangians and fast Fourier Transforms for composites with high contrast. CMES-Computer Modeling in Engineering & Sciences 1(2): 79–88.
- H. Moulinec, P. Suquet (1994) A fast numerical method for computing the linear and nonlinear mechanical properties of composites. Comptes Rendus De L Academie Des Sciences Serie Ii 318(11): 1417–1423.
- R.A. Lebensohn (2001) N-site modeling of a 3D viscoplastic polycrystal using Fast Fourier Transform. Acta Mater 49(14): 2723–2737.
- R. Brenner, R.A. Lebensohn, O. Castelnau (2009) Elastic anisotropy and yield surface estimates of polycrystals. Int J Solids Struct 46(16): 3018–3026.
- R.A. Lebensohn, R. Brenner, O. Castelnau, A.D. Rollett (2008) Orientation image-based micromechanical modelling of subgrain texture evolution in polycrystalline copper. Acta Mater 56(15): 3914–3926.

- R.A. Lebensohn, M.I. Idiart, P.P. Castaneda, P.G. Vincent (2011) Dilatational viscoplasticity of polycrystalline solids with intergranular cavities. Philos Mag 91(22): 3038–3067.
- A.K. Kanjarla, R.A. Lebensohn, L. Balogh, C.N. Tome (2012) Study of internal lattice strain distributions in stainless steel using a full-field elasto-viscoplastic formulation based on fast Fourier transforms. Acta Mater 60(6–7): 3094–3106.
- R.A. Lebensohn, A.K. Kanjarla, P. Eisenlohr (2012) An elasto-viscoplastic formulation based on fast Fourier transforms for the prediction of micromechanical fields in polycrystalline materials. Int J Plasticity 32–33: 59–69.
- P. Eisenlohr, M. Diehl, R.A. Lebensohn, F. Roters (2013) A spectral method solution to crystal elasto-viscoplasticity at finite strains. Int J Plasticity 46: 37–53.
- M.A. Kumar, I.J. Beyerlein, R.A. Lebensohn, C.N. Tome (2017) Modeling the effect of neighboring grains on twin growth in HCP polycrystals. Model Simul Mater Sc 25(6).
- M.A. Kumar, I.J. Beyerlein, R.A. Lebensohn, C.N. Tome (2017) Role of alloying elements on twin growth and twin transmission in magnesium alloys. Mat Sci Eng a-Struct 706: 295–303.
- M.A. Kumar, I.J. Beyerlein, C.N. Tome (2016) Grain size constraints on twin expansion in hexagonal close packed crystals. J Appl Phys 120(15).
- I.J. Beyerlein, R.J. McCabe, C.N. Tome (2011) Effect of microstructure on the nucleation of deformation twins in polycrystalline high-purity magnesium: A multi-scale modeling study. J Mech Phys Solids 59(5): 988–1003.
- R.F.S. Hearmon (1946) The Elastic Constants of Anisotropic Materials. Rev Mod Phys 18(3): 409–440.
- G. Simmons, H. Wang (year) Single crystal elastic constants and calculated aggregate properties: A Handbook. MIT Press.

- H. Abdolvand, A.J. Wilkinson (2016) Assessment of residual stress fields at deformation twin tips and the surrounding environments. Acta Mater 105: 219–231.
- L. Balogh, S.R. Niezgoda, A.K. Kanjarla, D.W. Brown, B. Clausen, W. Liu, C.N. Tome (2013) Spatially resolved in situ strain measurements from an interior twinned grain in bulk polycrystalline AZ31 alloy. Acta Mater 61(10): 3612–3620.
- I. Basu, H. Fidder, V. Ocelik, J.T.M. de Hosson (2018) Local Stress States and Microstructural Damage Response Associated with Deformation Twins in Hexagonal Close Packed Metals. Crystals 8(1).
- 38. Q. Sun, X. Zhang, Y. Ren, L. Tan, J. Tu (2015) Observations on the intersection between 1012 twin variants sharing the same zone axis in deformed magnesium alloy. Mater Charact 109: 160–163.
- Q. Sun, X.Y. Zhang, J. Tu, Y. Ren, H. Qin, Q. Liu (2015) Characterization of basal-prismatic interface of {1012} twin in deformed titanium by high-resolution transmission electron microscopy. Phil Mag Lett 95(3): 145–151.
- F. Wang, K. Hazeli, K.D. Molodov, C.D. Barrett, T. Al-Samman, D.A. Molodov, A. Kontsos, K.T. Ramesh, H. El Kadiri, S.R. Agnew (2018) Characteristic dislocation substructure in {1012} twins in hexagonal metals. Scripta Mater 143: 81–85.
- Y. Liu, N. Li, M.A. Kumar, S. Pathak, J. Wang, R.J. McCabe, N. A. Mara, C.N. Tome (2017) Experimentally quantifying critical stresses associated with basal slip and twinning in magnesium using micropillars. Acta Mater 135: 411–421.
- J. Jeong, M. Alfreider, R. Konetschnik, D. Kiener, S. Oh (2018) In-situ TEM observation of {1012} twin-dominated deformation of Mg pillars: Twinning mechanism, size effects and rate dependency. Acta Mater 158: 407–421.